# Secondary instability of plane channel flow to subharmonic threedimensional disturbances

Thorwald Herbert

Citation: Physics of Fluids (1958-1988) **26**, 871 (1983); doi: 10.1063/1.864226
View online: http://dx.doi.org/10.1063/1.864226
View Table of Contents: http://scitation.aip.org/content/aip/journal/pof1/26/4?ver=pdfcov
Published by the AIP Publishing

# LETTERS

*The purpose of this Letters section is to provide rapid dissemination of important new results in the fields regularly covered by The Physics of Fluids. Results of extended research should not be presented as a series of letters in place of comprehensive articles. Letters cannot exceed three printed pages in length, including space allowed for title, figures, tables, references and an abstract limited to about 100 words.*

## Secondary instability of plane channel flow to subharmonic three-dimensional disturbances

Thorwald Herbert
*Department of Engineering Science and Mechanics, Virginia Polytechnic Institute and State University, Blacksburg, Virginia 24061*

(Received 20 December 1982; accepted 27 January 1983)

A linear secondary instability mechanism is presented that leads to the occurrence of subharmonic three-dimensional disturbances in wall-bounded shear flows. The instability originates from the periodic redistribution of vorticity in the shear flow by small but finite-amplitude Tollmien–Schlichting waves. Low threshold amplitudes and other characteristics of this instability are consistent with experiments and may elucidate various obscure observations.

Recently, combined hot-wire measurements and flow visualizations in carefully controlled experiments[1–4] at low noise levels have shown that different paths can lead from initially two-dimensional Tollmien–Schlichting (T–S) waves to transition in wall-bounded shear flows. These paths are distinguished by the nature of secondary, three-dimensional disturbances that result in different characteristic patterns of $\Lambda$-shaped vortex loops in flow photographs, as sketched in Fig. 1. The commonly observed path[5,6] leads to spanwise alternating "peaks" and "valleys," i.e., regions of enhanced and reduced disturbance amplitude, that are associated with a mean longitudinal vortex system. The $\Lambda$ vortices are aligned along the peaks and repeat with the wavelength $\lambda_x$ of the T–S wave [Fig. 1(a)]. The peak–valley splitting originates from a secondary instability mechanism[7,8] that provides strong growth on a convective time scale if the maximum $u'_m$ of the streamwise r.m.s. fluctuation $u'$ exceeds a threshold of about 1% of the reference velocity. At even lower fluctuation levels, a different type of three-dimensionality can occur. In this case, flow visualization shows a staggered arrangement of $\Lambda$ vortices [Fig. 1(b)]. Obviously, the pattern repeats itself with wavelength $2\lambda_x$ and a fixed hot wire records subharmonic signals. It is tempting to attribute this suharmonic phenomenon to Craik's mechanism[9] that predicts resonance of certain wave triads for a specific spanwise wavelength $\lambda_z^*$. Some observations[2,3] are indeed consistent with Craik's model; others,[1,4] however, show different wavelengths $\lambda_z \neq \lambda_z^*$ under very similar experimental conditions. Moreover, Craik's mechanism is inoperative in plane Poiseuille flow by reasons of symmetry[10] but staggered $\Lambda$ vortices were recently observed in this flow.[4]

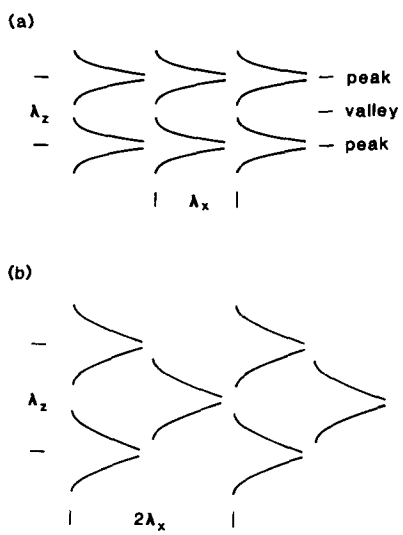


FIG. 1. Pattern of $\Lambda$ vortices in streakline photographs arising from three-dimensional secondary instability. (a) Ordered peak-valley structure with wavelength $\lambda_x$. (b) Staggered pattern with wavelength $2\lambda_x$. The flow is from left to right.

In this letter, we present a new mechanism that predicts strong linear instability to subharmonic three-dimensional disturbances without resorting to Craik's model. Whereas staggered $\Lambda$ vortices have been observed mostly in boundary layers, we present the theory for plane Poiseuille flow between parallel plates, driven by a pressure gradient in the $x$ direction. The reason for this choice is the existence of strictly periodic, two-dimensional wave solutions to the Navier–Stokes equations[11,12] in a moving frame,

$$\mathbf{v}_2(x,y,t) = \mathbf{v}_2(\xi,y), \quad \xi = x - ct, \tag{1}$$

where $c$ is the phase velocity, $t$ is the time, and $y$ is the coordinate normal to the walls at $y = \pm 1$. The wavelength in the streamwise direction $x$ or $\xi$ is $\lambda_x = 2\pi/\alpha$. Existence of these solutions is restricted to the neutral surface[12] defined by a

 0031-9171/83/040871-04$01.90  

nonlinear dispersion relation $F(A^2,R,\alpha,c) = 0$, where $A$ measures the fluctuation amplitude in terms of $u'_m$ and $R$ is the Reynolds number based on the channel half-width and the centerline velocity in the parabolic flow. Introducing a stream function $\psi$, the periodic solutions (1) can be written as

$$\psi(\xi,y) = \Psi(y) + A \sum_{n=-\infty}^{\infty} \phi_n(y) e^{in\alpha\xi}, \tag{2}$$

where $\Psi(y)$ represents the parabolic velocity profile $1 - y^2$. For real $\psi$, $\phi_{-n} = \tilde{\phi}_n$, where the tilde denotes the complex conjugate. Moreover, $\phi_n(-y) = (-1)^{n+1}\phi_n(y)$ due to the symmetry of plane Poiseuille flow and for consistency with the principal mode of T–S instability in the limit $A \to 0$.

Superposition of small, three-dimensional disturbances in the form

$$\mathbf{v}(\xi,y,z,t) = \mathbf{v}_2(\xi,y) + \epsilon \mathbf{v}_3(\xi,y,z,t) \tag{3}$$

leads, after linearization in $\epsilon$, to disturbance equations with coefficients independent of $z$ and $t$. We therefore assume disturbances in the form

$$\mathbf{v}_3(\xi,y,z,t) = e^{st} e^{i\beta z} \mathbf{f}(\xi,y), \tag{4}$$

where $\beta = 2\pi/\lambda_z$ is the spanwise wavenumber and $s = \sigma + i\omega$ combines the amplification rate $\sigma$ and the frequency $\omega$ with respect to a frame moving with $c$.

The resulting disturbance equations have periodic coefficients owing to the periodic base flow (2). Apart from the $y$ dependence, the equations are essentially of the Hill type (or Mathieu type) with damping. Such systems permit various classes of solutions; the two most important classes arise from primary (fundamental) resonance with wavelength $\lambda_x$ and from principal parametric (subharmonic) resonance with wavelength $2\lambda_x$. Primary resonance generates the modes of instability[7,8] that are associated with peak–valley splitting. In plane Poiseuille flow, two groups of such modes are distinguished by different symmetry in the $y$ direction. For principal parametric resonance one obtains disturbances (4) with

$$\mathbf{f}(\xi,y) = \sum_{m=-\infty}^{\infty} \mathbf{f}_{2m+1}(y) e^{i(2m+1)\alpha\xi/2}. \tag{5}$$

Beyond being doubly periodic with $\lambda_z$ and $2\lambda_x$, these disturbances are invariant under the translation $(\xi,z) \to (\xi + \lambda_x, z + \lambda_z/2)$ that is characteristic for the staggered pattern in Fig. 1(b). Due to the absence of aperiodic terms in the series (5), the disturbances cannot lead to a mean longitudinal vortex system. In plane Poiseuille flow, the functions $\mathbf{f}_{2m+1}(y)$ for even and odd $m$ have opposite symmetry in $y$. Consequently, $\mathbf{f}$ itself is asymmetric and the distinction of modes with different $y$ symmetry is redundant. With homogeneous boundary conditions for the components of $\mathbf{f}$ one obtains an eigenvalue problem for $s$. After truncating the Fourier series (2) and (5) we have applied a Chebyshev-collocation technique[13] in $y$ for solving this problem numerically. The results given below are for the symmetry $u_1(y) = u_1(-y)$ and for the lowest consistent approximation $|n| \leqslant 1$ in Eq. (2), $m = -1, 0$ in Eq. (5). Eliminating the spanwise velocity components and using 18 collocation points in $0 \leqslant y \leqslant 1$ results in a $78 \times 78$ complex matrix eigenvalue problem for $s$. The eigenvectors provide the velocity components

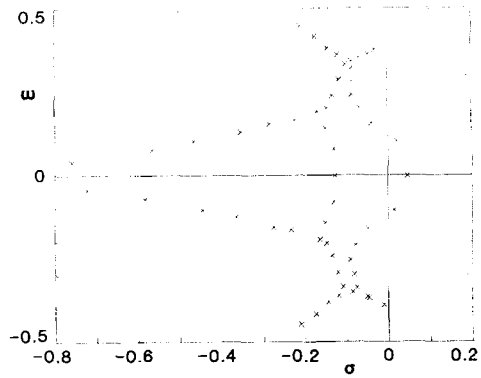


FIG. 2. Spectrum of eigenvalues $s = \sigma + i\omega$ with $\sigma > -0.8$ of subharmonic modes at $R = 5000$, $\alpha = 1.12$, and $\beta = 2.0$, where $A = 0.0248$.

$u_1, u_{-1}$ (streamwise) and $v_1, v_{-1}$ (normal to the walls) whereas $w_1, w_{-1}$ can be retrieved from the continuity equation.

Figure 2 shows the spectrum of eigenvalues $s$ in a cutout of the complex domain for $R = 5000$, $\alpha = 1.12$, and $\beta = 2.0$. These parameters are close to experimental situations.[4,6] The periodic basic flow (2) has $A \simeq 0.025$ for this point. The asymmetry of the spectrum about the real axis reflects the lacking symmetry of $\mathbf{f}(\xi,y)$ in Eq. (5). There are three eigenvalues in the right half-plane, $\sigma > 0$, that can lead to instability. The dominant mode of subharmonic instability is associated with $s = 0.0465 - i\,0.0020$. This eigenvalue is slightly off the real axis, indicating that three-dimensional and two-dimensional disturbances travel at slightly different speed. The instability is strong in the sense that the subharmonic disturbance grows by a factor of 100 within about five cycles of the T–S wave. The growth rate is very similar to that found for primary resonance at these parameters.[8] This is not surprising since the strong mechanism of combined vortex stretching and tilting[7] is common to both types of instability. Similar results were also found[14] for the three-dimensional subharmonic (helical pairing) and fundamental (translative) modes of instability in a periodic shear layer.

Figure 3 shows $\sigma$ and $\omega$ for the dominant mode at $R = 5000$ and $\alpha = 1.12$ as functions of the spanwise wavenumber $\beta$. The growth rate $\sigma$ has a maximum at $\beta \simeq 1.26$ and decreases almost linearly with increasing $\beta$ owing to increasing dissipation. For $\beta < 1$, $\sigma$ rapidly decreases with decreasing $\beta$, while the frequency shift $|\omega|$ between subharmonic disturbances and basic flow increases. This shift can be related to the frequently observed low-frequency phenomena[15] at onset of three-dimensionality and to the broad subharmonic peak in disturbance spectra. The instability is cut off at low $\beta$, indicating suppression of the two-dimensional pairing mode[14] in the neighborhood of a wall.

Variation of the dominant eigenvalue with the amplitude $A$ is shown in Fig. 4 for $\alpha = 1.02$ and $\beta = 2.0$. Strictly periodic basic flows of different amplitude are obtained by varying $R$ between $R_c = 5772$ $(A = 0)$ and $R \simeq 5100$ $(A = 0.02)$, where $A^2 \sim R_c - R$. As $A$ decreases, the growth rate decreases and changes sign at a threshold amplitude $A_s \simeq 0.0066$. Below this threshold, the periodic vorticity concentration is too feeble to overcome viscous damping,

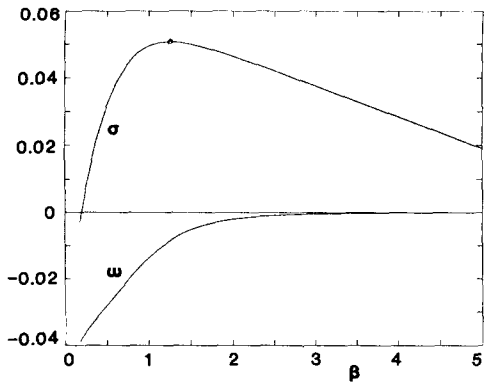


FIG. 3. Amplification rate $\sigma$ and relative frequency $\omega$ for the dominant mode of subharmonic instability as a function of $\beta$ at $R = 5000$ and $\alpha = 1.12$. The maximum of $\sigma$ is marked by 0.

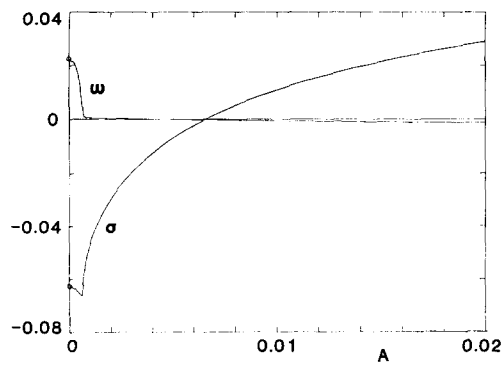


FIG. 4. Amplification rate $\sigma$ and relative frequency $\omega$ for the dominant mode of subharmonic instability as a function of the amplitude $A$ at $\alpha = 1.02$ and $\beta = 2.0$.

and the subharmonic disturbance suffers strong decay at lower amplitudes. For $\alpha = 1.02$, the lowest threshold is $A_s \simeq 0.0042$ at $\beta \simeq 0.74$, whereas the lowest threshold for peak–valley splitting is $A_f \simeq 0.0085$ at $\beta \simeq 1.22$. For $\beta = O(1)$, we can distinguish three amplitude ranges that may be relevant for the interpretation of experiments: (i) $0 \leqslant A \leqslant A_s$, no three-dimensional instability; (ii) $A_s < A \leqslant A_f$, instability to subharmonic modes, with considerable growth rates as $A \to A_f$; and (iii) $A_f < A$, instability to both types of three-dimensional disturbances. The appearance of the one or the other type (or a mixture of both) depends largely on the background disturbances. A glance at various experiments in boundary layers has not revealed any inconsistency with these theoretical predictions.

As $A \to 0$ in Fig. 4, the eigenvalue $s$ tends to an eigenvalue $s_1$ of the classical linear stability problem for three-dimensional disturbances in plane Poiseuille flow. It is worthy of note that $s_1 = -0.0626 + i\,0.0225$ is not an eigenvalue of the Orr–Sommerfeld problem. Instead, $s_1$ is an eigenvalue of the second-order differential equation for $u_1$ for the special case of $v_1 \equiv 0$.[16] The peculiar variation of $s$ in the neighborhood of $A = 0$ is due to interaction of the two eigenvalues $s_1$ and $s_{-1} \simeq \tilde{s}_1$, where $s_{-1}$ is an eigenvalue of the homogeneous equation for $u_{-1}$. The mode originating from $s_{-1}$ suffers strong decay as $A$ increases.

For $\beta$ sufficiently large, the subharmonic disturbances retain the property $v_{\pm 1} \simeq 0$ at finite amplitudes $A$. (The rise of the $v$ components seems to be associated with the rise of a frequency shift, $|\omega| \neq 0$, at smaller values of $\beta$.) Assuming $v \equiv 0$ provides the approximations

$$w_{\pm 1} \simeq \mp(\alpha/2\beta)u_{\pm 1}, \quad \eta_{\pm 1} \simeq i\beta\,[1 + (\alpha/2\beta)^2]u_{\pm 1}, \quad (6)$$

where $\eta$ denotes the $y$ component of vorticity. The normalized distributions $u'/u'_m$ vs $y$ for the two-dimensional fundamental and for the subharmonic are shown in Fig. 5. The shape of the subharmonic profile and the position of its maximum with respect to the critical layer of the T–S wave are consistent with experiments in the flat-plate boundary layer.[1,3] This evidence is stronger than it seems at first glance: the data in Fig. 5 are representative for the dominant mode of subharmonic instability at different spanwise positions $z$ and different wavenumbers $\beta$. As long as $\sigma > 0$, the picture experiences no significant change by varying the wavenumber $\alpha$ or the amplitude $A$ of the basic flow.

For $\omega t = 0$, the extrema of $u$ and $\eta$ according to Eq. (6) for the subharmonic disturbance coincide with the maxima of the basic-flow stream function $\psi(\xi,y)$ that are spaced $\lambda_x$ apart and close to the wall at $y = 1$. The redundant mode of different symmetry that can be obtained by the transformation $(\xi,y) \to (\xi + \lambda_x/2, -y)$ is obviously associated with the minima of $\psi$ along the opposite wall in Poiseuille flow. This coincidence reveals the simple mechanism of the subharmonic instability[17]: the extrema of $\psi$ represent material-bound line vortices; the spanwise periodic $\eta$ disturbance bends these vortices in the $y,z$ plane into regions of different streamwise velocity, where stretching completes the growth of the disturbances on a fast convective time scale. Nonlinear development will rapidly take over and lead to transition. Curiously, a single mode of subharmonic instability initiates transition in the neighborhood of only one of the two channel walls at a time.

This investigation was stimulated by discussions on experimental results with William S. Saric, Victor Ya. Levchenko, and Victor V. Kozlov.

The work was supported by the National Science Foundation under Grant No. MEA 81-20935.

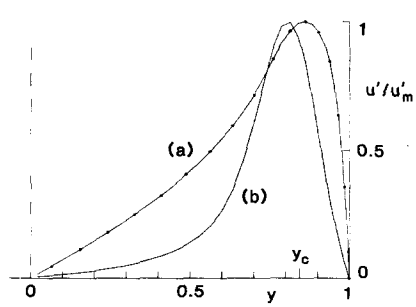


FIG. 5. Normalized distributions $u'/u'_m$ as a function of $y$ for the basic flow (a) and for the subharmonic disturbance (b) at $R = 5000$, $\alpha = 1.12$, and $\beta = 2.0$. The critical layer of the basic flow is located at $y_c$.

[1]A. S. W. Thomas and W. S. Saric, Bull. Am. Phys. Soc. **26**, 1252 (1981).
[2]W. S. Saric, J. D. Carter, and G. A. Reynolds, Bull. Am. Phys. Soc. **26**, 1252 (1981).
[3]Yu. S. Kachanov and V. Ya. Levchenko, I.T.A.M., USSR AN Novosibirsk, Preprint 10-82, 1982.
[4]V. V. Koslov (personal communication, partly published); V. V. Kozlov and M. P. Ramasanov, I.T.A.M., USSR AN Novosibirsk, Preprint 4-82, 1982.
[5]P. S. Klebanoff, K. D. Tidstrom, and L. M. Sargent, J. Fluid Mech. **12**, 1 (1962).
[6]M. Nishioka, M. Asai, and S. Iida, in *Laminar-Turbulent Transition*, edited by R. Eppler and H. Fasel (Springer-Verlag, Berlin, 1980), p. 37.
[7]S. A. Orszag and A. T. Patera, in *Transition and Turbulence*, edited by R. E. Meyer (Academic, New York, 1981), p. 127.
[8]Th. Herbert, Bull. Am. Phys. Soc. **26**, 1257 (1981); and Report No. VPI-E-81-35, 1981.
[9]A. D. D. Craik, J. Fluid Mech. **50**, 393 (1971).
[10]Th. Herbert and M. V. Morkovin, in *Laminar-Turbulent Transition*, edited by R. Eppler and H. Fasel (Springer-Verlag, Berlin, 1980), p. 47.
[11]J. P. Zahn, J. Toomre, E. A. Spiegel, and D. O. Gough, J. Fluid Mech. **64**, 319 (1974).
[12]Th. Herbert, AGARD CP-224, Paper No. 3, 1977; Th. Herbert, Habilitationsschrift, Universität Stuttgart, 1978.
[13]Th. Herbert, "Three-dimensional Instability of Periodic Secondary Motions in a Plane Channel" (to be published).
[14]R. T. Pierrehumbert and S. E. Widnall, J. Fluid Mech. **114**, 59 (1982).
[15]W. S. Saric and G. A. Reynolds, in *Laminar-Turbulent Transition*, edited by R. Eppler and H. Fasel (Springer-Verlag, Berlin, 1980), p. 125.
[16]H. B. Squire, Proc. R. Soc. London Ser. A **142**, 621 (1933).
[17]In a heuristic manner, such a mechanism has been employed for an interpretation of streakline photographs by F. X. Wortmann, in *Advances in Fluid Mechanics, Lecture Notes in Physics* (Springer-Verlag, Berlin, 1981), Vol. 148, p. 268.

# Separation of time-averaged turbulence components by laser-induced fluorescence

S. Cheng, M. Zimmermann, and R. B. Miles
*Department of Mechanical and Aerospace Engineering, Princeton University, Princeton, New Jersey 08544*

(Received 4 October 1982; accepted 20 January 1983)

Turbulence is measured by resonant fluorescence of sodium atoms seeded into a supersonic nitrogen jet. By varying the frequency of the pumping laser, the mean square velocity, temperature, and pressure fluctuations (as well as their correlations) may be determined.

Turbulence measurements in flowing gases have until now been performed primarily with hot-wire techniques[1] and laser Doppler velocimetry (LDV).[2] These measurements are particularly difficult in supersonic flows where high-turbulence frequencies are encountered and fluctuations in all the fluid properties are of interest. In hot-wire anenometry, very thin wires (five microns diameter or less)[3] are used to follow variations in the flow. The length of these wires (approximately 1 mm) seriously restricts the spatial resolution[4] and the practical limit of the frequency response is lower than the highest frequencies of interest in supersonic flows. Moreover, the measurements cannot uniquely distinguish velocity fluctuations from density fluctuations. The LDV technique is also of limited utility in supersonic flows because of the inability of the particles to follow high-frequency flow fluctuations.[5] In addition to these techniques laser-induced fluorescence has been used recently to time resolve relative density fluctuations.[6,7]

Here we report the first use of the Resonant Doppler Velocimeter (RDV) to observe time-averaged turbulence fluctuations. We demonstrate that, by the proper choice of laser frequency, velocity fluctuations may be removed from the fluorescence signal or, alternatively, selected components of the turbulence may be highlighted. By recording the turbulence spectrum at a variety of laser frequencies the relative contribution of each fluid property as well as the correlations between these properties may be determined.

The Resonant Doppler Velocimeter has thus far been used for flow visualization and for quantitative measurements of the average velocity, temperature and pressure of a gaseous flow.[8] This is achieved by shining a single-frequency laser beam into a flow which is seeded with an atomic or molecular species. The laser is tuned through the absorption frequency of the seeded species and the resulting fluorescence is monitored by a detector. The velocity component in the direction of the laser beam can be determined by observing the Doppler shift of the absorption frequency, and spectroscopic absorption line broadening mechanisms furnish information regarding the static temperature and pressure of the moving gas.

The laser-induced fluorescence intensity $I_\nu$ for an optical depth much smaller than one is given by[9]

$$I_\nu = I_L \kappa_\nu \Delta x. \tag{1}$$

The laser intensity $I_L$ is assumed independent of frequency $\nu$ and $\Delta x$ is the length of the volume of interest along the laser beam. The fluorescence intensity depends on the velocity, temperature, and pressure since the absorption coefficient $\kappa_\nu$ for laser intensities much lower than the saturation intensity is given by[9]

$$\kappa_\nu = \pi r_0 f_{12} \frac{p}{kT}\left(\int_{-\infty}^{\infty}\left(\frac{1}{\pi}\frac{\Delta\nu_L}{(\nu-\nu_{12}-\Delta)^2+(\Delta\nu_L)^2}\right)\times\left\{\left(\frac{\ln 2}{\pi}\right)^{1/2}\frac{1}{\Delta\nu_G}\exp\left[-\ln 2\left(\frac{\Delta}{\Delta\nu_G}\right)^2\right]\right\}d\Delta\right). \tag{2}$$

Here $r_0 = 2.82\times10^{-15}$ m, $f_{12}$ is the absorption oscillator strength, $p$ is the pressure, $k$ is Boltzmann's constant, $T$ is the

 0031-9171/83/040874-04$01.90  